ACS OMEGA

http://pubs.acs.org/journal/acsodf

Article

Topical Application of 4′-Hydroxychalcone in Combination with *tt*-Farnesol Is Effective against *Candida albicans* and *Streptococcus mutans* Biofilms

Carmélia I. Lobo, Paula A. Barbugli, Guilherme Roncari Rocha, and Marlise I. Klein*

Cite This: *ACS Omega* 2022, 7, 22773−22786

Read Online

ACCESS | Metrics & More | Article Recommendations | Supporting Information

ABSTRACT: *Candida albicans* and *Streptococcus mutans* interaction in the presence of dietary sucrose yields a complex biofilm with an organized and structured extracellular matrix that increases the tolerance to environmental stress, including antimicrobials. Both species are found in severe early childhood caries lesions. Thus, compounds 4′-hydroxychalcone (C135) (flavonoid intermediate metabolites), *tt*-farnesol (Far) (terpenoid), and sodium fluoride (F) were tested either isolated or combined as topical treatments (5 min twice daily) against *C. albicans* and *S. mutans* dual-species biofilms grown on saliva-coated hydroxyapatite discs. The biofilms were evaluated for gene expression, microbial population, biochemical components, and three-dimensional (3D) structural organization via confocal microscopy and scanning electron microscopy (SEM). The cytotoxicity of formulations was tested on the keratinocyte monolayer. C135 + Far + F promoted lower gene expression of fungal genes associated with β-glucan synthesis (*BGL2*, *FKS1*) and remodeling (*XOG1*, *PHR1*, *PHR2*), oxidative stress (*SOD1*), and drug tolerance (*CDR1*, *ERG11*) and higher expression of bacterial *nox1* (oxidative and acidic stress tolerance). C135 + Far yielded less insoluble exopolysaccharides, biomass, and proteins (insoluble portion) and lower expression of *BGL2*, *ERG11*, *SOD1*, and *PHR2*. C135 + F, C135 + Far + F, and C135 rendered lower biomass, thickness, and coverage percentage (confocal microscopy). C135 + Far and C135 + Far + F maintained *C. albicans* as yeast morphology (SEM). Therefore, the formulations with C135 affected fungal and bacterial targets but exerted a more pronounced effect against fungal cells.

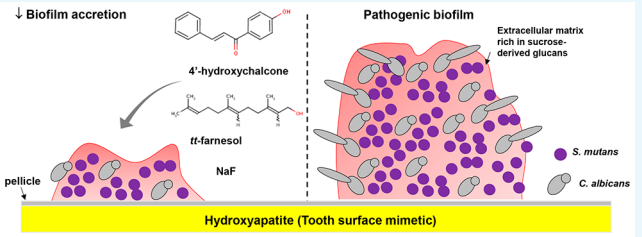

INTRODUCTION

Over time, organized biofilms in the oral cavity can lead to severe diseases with complex management, such as dental caries. Dental caries is a multifactorial disease affecting people of all social classes and ages.[1] Early childhood caries or ECC is a serious public health problem and is considered one of the most common preventable diseases affecting children. Its prevalence is related to the interaction of the type of microorganisms, diet, and caregivers' instruction.[2] Essentially, dental caries is a biofilm-diet-derived disease in which the organic acids from microbial metabolism are trapped inside the biofilm and at the interface biofilm/teeth surface by its extracellular matrix, leading to teeth demineralization,[3] which can result in teeth loss that affects oral and systemic health.[4]

Interaction of microorganisms, especially *Streptococcus mutans* and *Candida albicans*, makes a complex biofilm with an organized and structured extracellular matrix that contributes to increasing the environmental stress tolerance of both species.[5] This association appears to be primarily mediated by a physical interaction that relies on glucans produced by bacterial exoenzyme glucosyltransferases (Gtfs) on yeast and hyphal cell surfaces.[6] Gtfs convert a moderately cariogenic organism into a major contributor to the formation of virulent plaque biofilms and dental caries *in vivo*.[7]

The antimicrobial effect against microorganisms is usually compromised by their cell wall barrier and the extracellular matrix. *S. mutans* Gtfs synthesize exopolysaccharides (α-glucans) using dietary sucrose as the substrate for the extracellular matrix construction.[8] During biofilm development in the presence of a cariogenic diet, *S. mutans* genes related to biofilm's matrix construction (e.g., *gtfB*, *gtfC*, *gtfD*), acid production, tolerance to acids (e.g., *atpD*), and oxidative stresses (e.g., *nox1*) are expressed.[9−11] Also, the *C. albicans* cell wall has important components (β-glucans) that contribute to fungal virulence. Genes *BGL2*, *FKS1*, *PHR1*, and *XOG1* are related to β-1,3-glucan (and antifungal resistance) and β-1,6-glucan (*PHR1*) synthesis and are essential for the extracellular matrix construction.[12−14] In addition, genes *PHR1* and *PHR2* are expressed at imbalanced pH and contribute to acid production by *C. albicans* and its survival in acidic environments;[12] *SOD* and *ERG11* genes are related to oxidative

Received: April 13, 2022
Accepted: June 2, 2022
Published: June 22, 2022

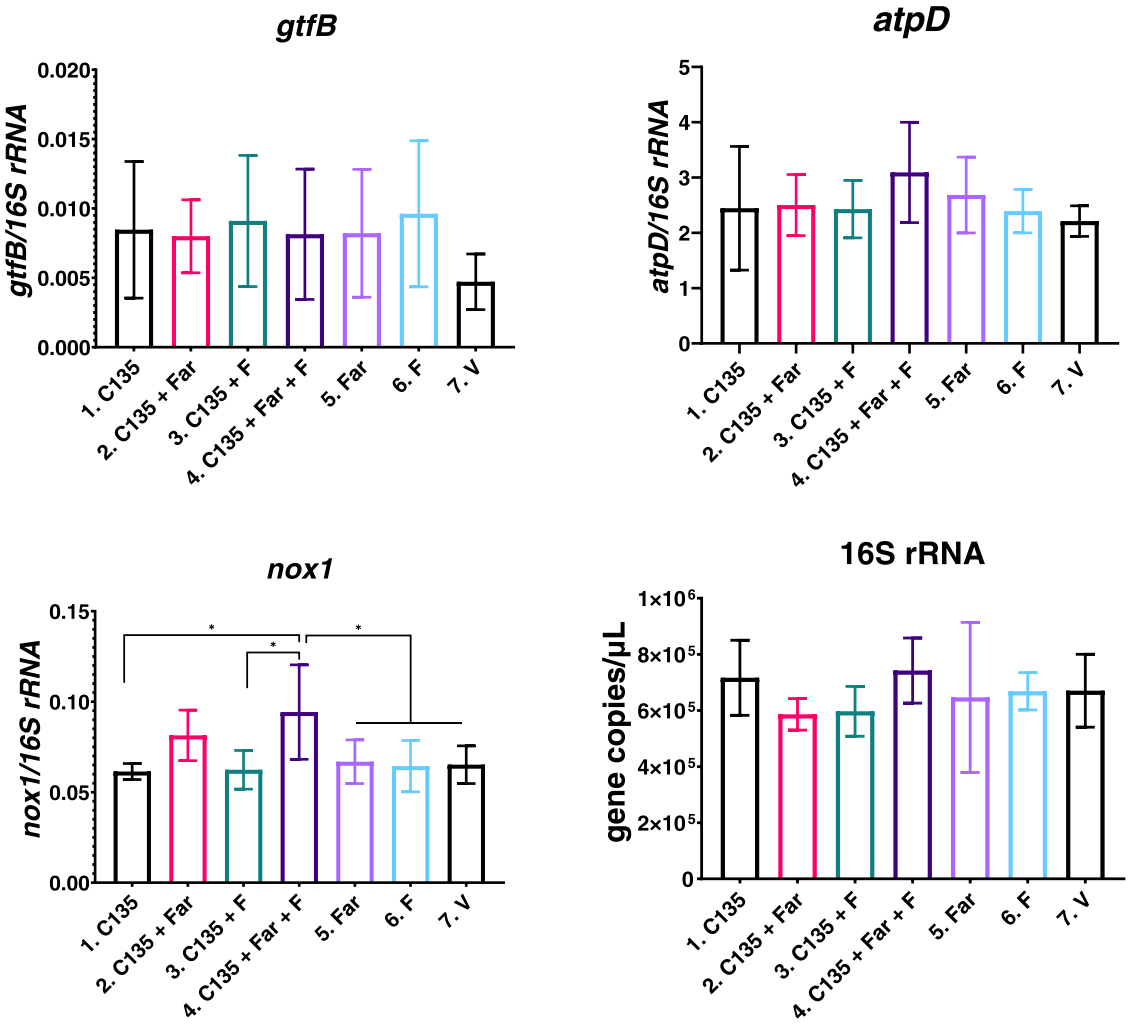

Figure 1. *S. mutans* gene expression of 28 h old *S. mutans* and *C. albicans* biofilms. Biofilms treated with C135, *tt*-farnesol (Far), and sodium fluoride (F) alone and in combination (1.C135; 2.C135 + Far; 3.C135 + F; 4.C135 + Far + F; 5.Far; 6.F) and 7.Vehicle or V. Data are represented as means and standard deviations (n = 3), where asterisks represent differences ($^*p \leq 0.0384$).

stresses, and *CDR*1 and *ERG*11 are associated with antimicrobial resistance.[15−17] In addition, the *ERG*11 gene is part of the ergosterol biosynthesis pathway, and it is related to the morphogenesis of the hyphal form and fungal virulence.[18]

Disrupting pathogenic local niches to eliminate the embedded microorganisms and facilitate access to the action of the agents by targeting the biofilm structure and its microenvironment can be an effective therapeutic strategy, especially if the agents generate minimal cytotoxicity and minimize the drug resistance issue.[19]

Fluoride and chlorhexidine digluconate are the gold standards for topical treatments of dental biofilms. Fluoride helps balance the remineralization process after demineralization,[20] enhancing remineralization in the presence of dental plaque. However, it has a limited effect on biofilms *per se*; it has a small action on glycolysis or acid production.[21] On the other hand, chlorhexidine is a broad-spectrum antimicrobial, important for Gram-positive bacteria control like *S. mutans*; nevertheless, its daily use is limited (up to 15 days).[22] Thus, treating cariogenic biofilms is still a public health challenge; hence, finding an alternative that could be used daily for cariogenic biofilm control for dental caries prevention becomes interesting.

Several compounds have been studied to serve as antimicrobial and antibiofilm strategies. Hydroxychalcones inhibited the Gtfs' activity of *S. mutans*.[23] Chalcones affect the cell wall formation of *C. albicans*, contributing to mitochondrial dysfunction and the efflux-mediated pumping system.[24] 4′-Hydroxychalcone (C135) presented promising effects against *C. albicans* and *S. mutans* growth in planktonic cultures and single- and dual-species biofilms after long exposure.[25] *tt*-Farnesol is a *C. albicans* quorum sensing molecule that hinders fungal filamentation (hyphal formation) and targets *S. mutans* cytoplasmatic membrane, affecting the bacterium stress tolerance and survival.[26] Myricetin is a flavonoid that interferes mainly with *S. mutans* exopolysaccharide production.[27]

Topical treatment using the association of *tt*-farnesol with myricetin and fluoride decreases the number of dental caries lesions; these lesions are less severe than the controls in rats colonized by *S. mutans*.[27] However, this formulation (*tt*-farnesol plus myricetin plus fluoride) applied topically (1.5 min) had little effect on *C. albicans* and *S. mutans* dual-species biofilms *in vitro*.[28] In addition, 24 h exposure to the combination of 4′-hydroxychalcone (C135) with *tt*-farnesol and fluoride hindered that dual-species biofilm development and killed both bacteria and fungi in the preformed biofilms

https://doi.org/10.1021/acsomega.2c02318
ACS Omega 2022, 7, 22773−22786

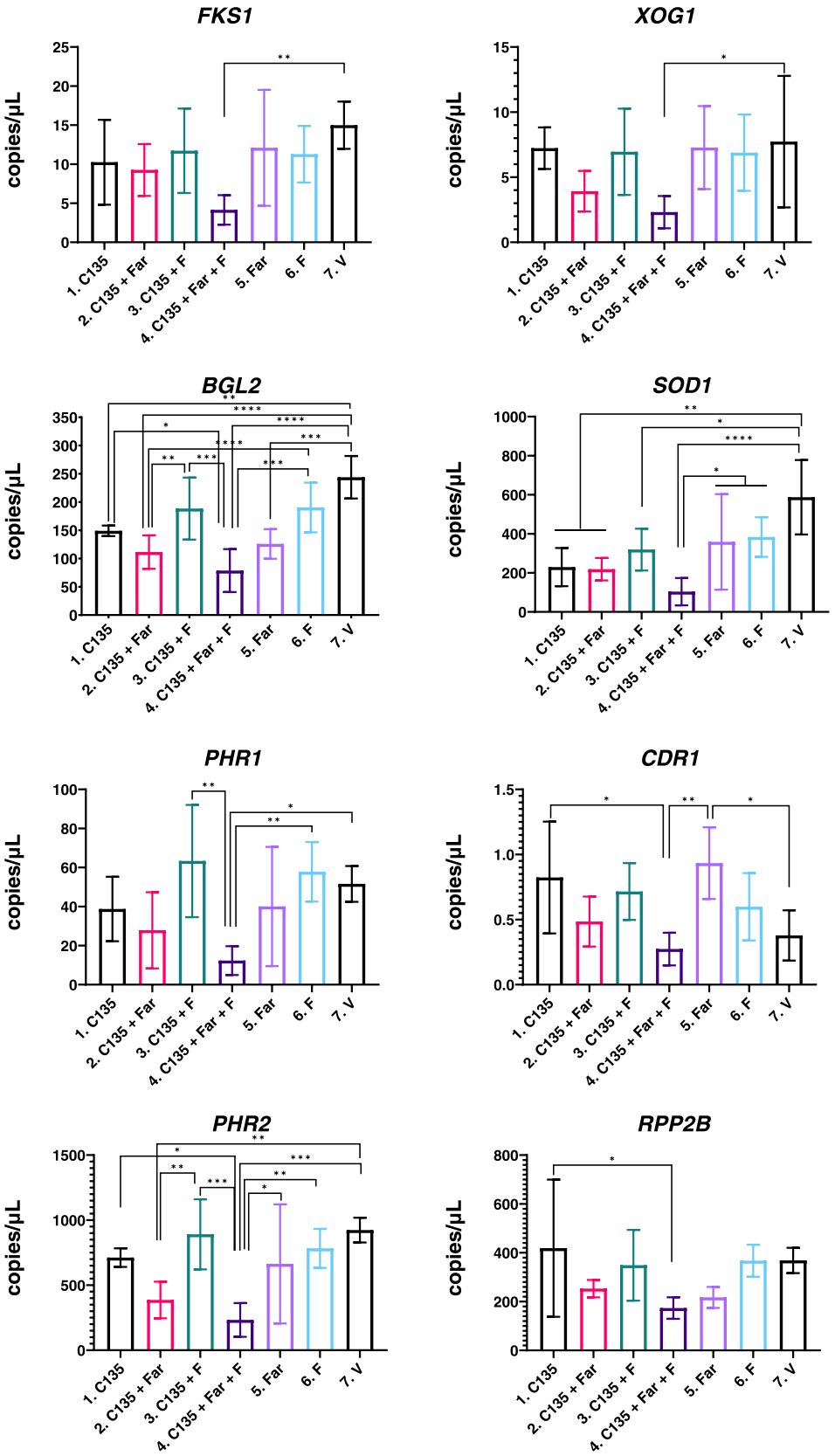

Figure 2. *C. albicans* gene expression of 28 h old *S. mutans* and *C. albicans* biofilms. Biofilms treated with C135, *tt*-farnesol (Far), and sodium fluoride (F) alone and in combination (1.C135; 2.C135 + Far; 3.C135 + F; 4.C135 + Far + F; 5.Far; 6.F) and 7.Vehicle or V. Data represent means and standard deviations (n = 3) from three different experiments. Differences are presented by asterisks: *$p \leq 0.0450$, **$p \leq 0.0060$, ***$p \leq 0.0006$, and ****$p \leq 0.0001$.

https://doi.org/10.1021/acsomega.2c02318
ACS Omega 2022, 7, 22773−22786

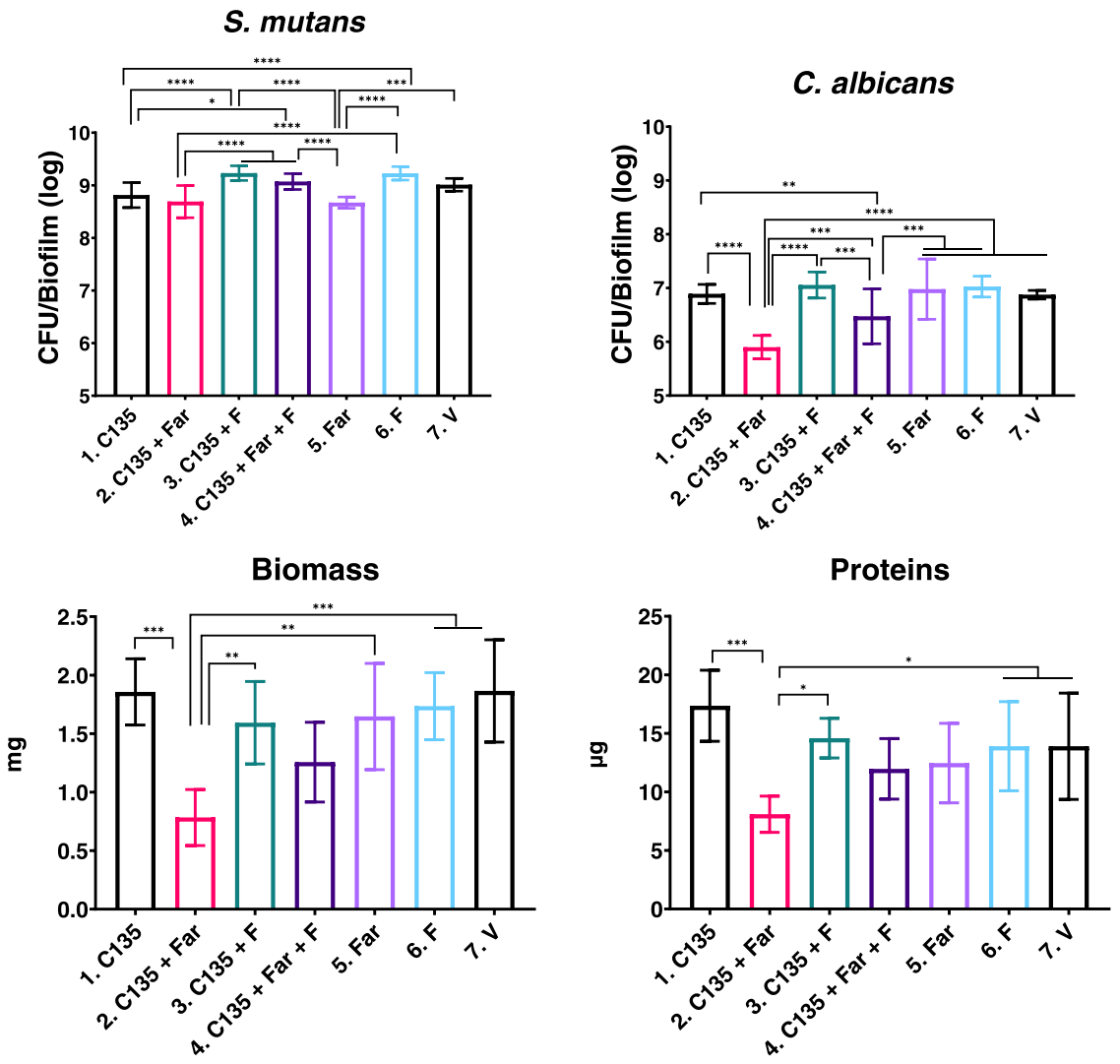

Figure 3. Overall biofilm features of 43 h old *S. mutans* and *C. albicans* dual-species biofilms. The graphs depict microbial population, biomass (dry weight), and proteins (in the insoluble portion). Biofilms treated with C135, *tt*-farnesol (Far), and sodium fluoride (F) alone and in combination (1.C135; 2.C135 + Far; 3.C135 + F; 4.C135 + Far + F; 5.Far; 6.F) and 7.Vehicle or V. Data represent means and standard deviations ($n = 6$) and differences are represented by asterisks: *$p \leq 0.0396$, **$p \leq 0.0056$, ***$p \leq 0.001$, and ****$p \leq 0.0007$.

(96-well polystyrene plates model).[25] Nonetheless, further research is needed to pinpoint formulations for effective topical treatments to control fungal−bacterium biofilms.

Therefore, finding a formulation with an effective combination of compounds for topical application to prevent *S. mutans* and *C. albicans* biofilm development may result in a strategy to prevent dental caries lesions. Here, the promising agents (4′-hydroxychalcone and *tt*-farnesol)[25] and their combinations with and without fluoride were tested as topical treatments against dual-species biofilms formed on saliva-coated hydroxyapatite (HA) discs.

RESULTS

Gene Expression. The data on *S. mutans* genes (*atpD*, *gtfB*, and *nox*1) were normalized by 16S rRNA (Figure 1). The expression of *nox*1 was higher (*versus* other groups) for biofilms treated with C135 + Far and C135 + Far + F, but statistical difference *versus* vehicle was found for C135 + Far + F (one-way ANOVA: $p = 0.003$; Tukey's post-test $p = 0.0238$). Significant statistical differences were also observed for C135 + Far + F versus C135, Far, and F ($p \leq 0.0384$) for this gene. However, no differences were observed for *atpD* and *gtfB* gene expression ($p \geq 0.5688$).

The eight *C. albicans* genes analyzed were *BGL2*, *ERG11*, *CDR1*, *FKS1*, *PHR1*, *PHR2*, *RPP2B*, *SOD1*, and *XOG1* (Figure 2). Gene *RPP2B* was selected as a normalizer gene for *C. albicans*, but because of statistical differences in C135 *versus* C135 + Far + F (one-way ANOVA: $p = 0.0187$; Tukey's post-test: $p = 0.0322$), this gene did not work as a normalizer. A lower fungal gene expression was observed for all genes when all compounds were combined (C135 + Far) with or without sodium fluoride.

Specifically, for *BGL2* (a cell wall 1,3 β-glucosyltransferase associated with cell wall biosynthesis),[14] the lowest expression values were observed for C135 + Far + F (*vs* C135, C135 + F, F, and V; $p \leq 0.0341$) and for C135 + Far (*vs* C135 + F, F, and V; $p \leq 0.0149$). Besides, a lower expression for *BGL2* was quantified for C135 and Far *versus* vehicle ($p \leq 0.0016$). A similar gene expression profile was observed for *ERG11* (important for ergosterol synthesis, morphogenesis, and virulence of *C. albicans*)[16,18] with significative statistical

https://doi.org/10.1021/acsomega.2c02318
ACS Omega 2022, 7, 22773−22786

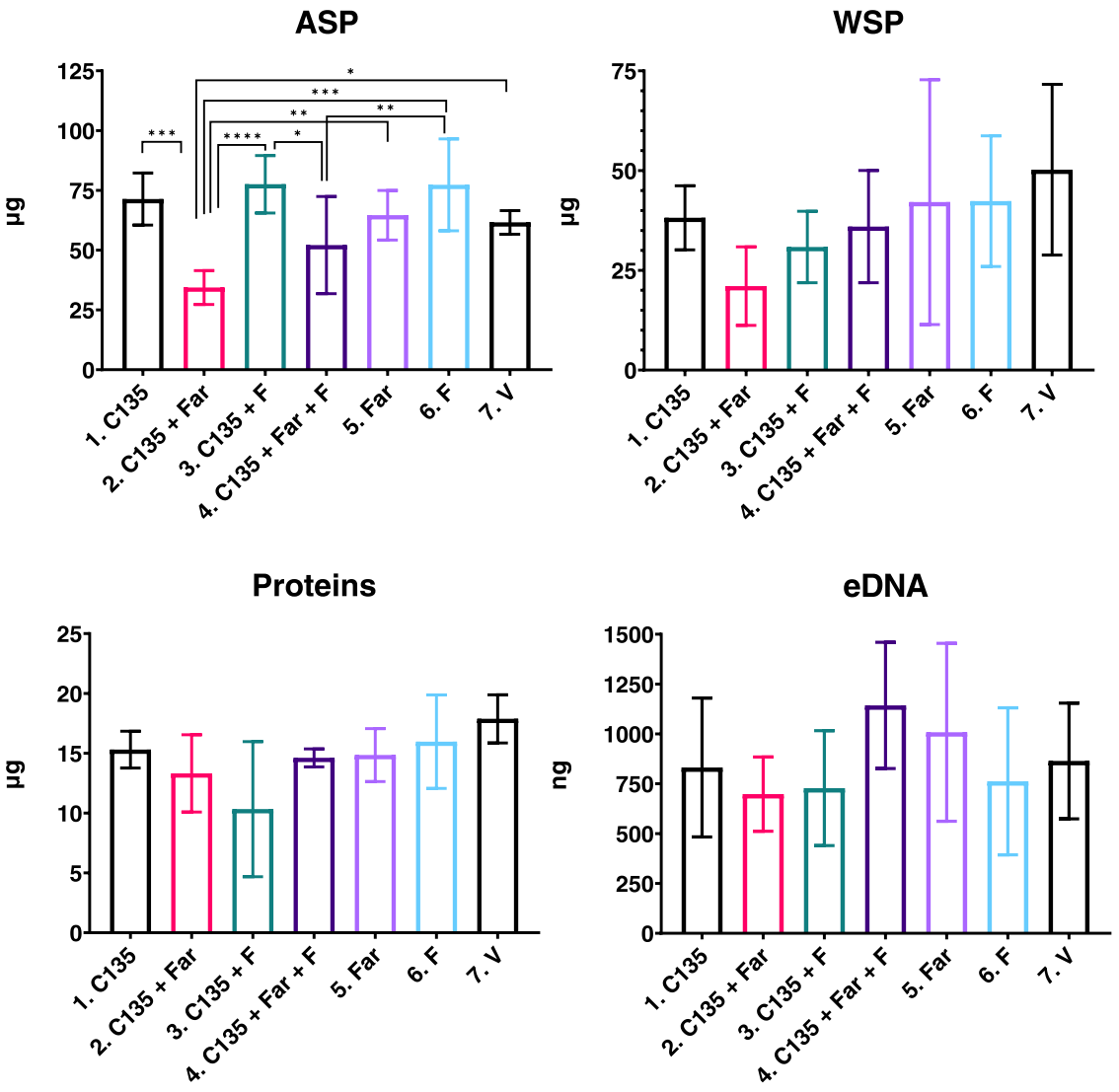

Figure 4. Extracellular matrix components of 43 h old *S. mutans* and *C. albicans* dual-species biofilms. The graphs depict exopolysaccharides (ASP and WSP), proteins (from the soluble portion), and eDNA. Biofilms treated with C135, *tt*-farnesol (Far) and sodium fluoride (F) alone and in combination (1.C135; 2.C135 + Far; 3.C135 + F; 4.C135 + Far + F; 5.Far; 6.F) and 7.Vehicle or V. Data represents means and standard deviations (n = 6). Asterisks represent differences: **$p \leq 0.0051$ and ***$p \leq 0.0007$.

differences for C135, C135 + Far, and C135 + Far + F *versus* vehicle ($p \leq 0.0404$).

*FKS*1 (an essential β-1,3-glucan synthase subunit) and *XOG*1 (exo-1,3 β-glucanase), important genes for the matrix construction,[14] presented a reduced expression in biofilms treated with C135 + Far + F *versus* vehicle ($p = 0.0467$ and $p = 0.0046$, respectively). In addition, *CDR*1 (a multidrug transporter of the ABC superfamily) exhibited lower gene expression for C135 + Far + F *versus* C135 and Far; there was also a difference in Far *versus* V ($p \leq 0.0244$).

*PHR*1 (a cell surface glucosidase) presented significant differences between C135 + Far + F *versus* C135 + F, F, and vehicle ($p \leq 0.0248$). At the same time, the expression of *PHR*2 (a glucosidase) for all treatment groups was higher than C135 + Far + F ($p < 0.0001$), except for C135 + Far ($p = 0.8966$).

Besides, *SOD*1 (a superoxide dismutase gene) showed a lower gene expression in all treatments containing C135 (C135, C135 + Far, C135 + F, and C135 + Far + F) than the vehicle; in addition, C135 + Far + F presented lower expression *versus* Far and F ($p \leq 0.0450$).

Microbial Population. After treatments, the viable microbial population was different between *S. mutans* and *C. albicans* (Figure 3). *S. mutans* population presented significant statistic differences for C135 (*vs* C135 + F and F), C135 + Far (*vs* C135 + F, C135 + Far + F, and F), and Far (*vs* C135 + Far + F, C135 + F and F) ($p \leq 0.0396$). Biofilms treated with C135, Far, or both compounds in combination (C135 + Far) reduced microbial populations more than fluoride formulations. Besides, C135 + Far and Far yielded lower *S. mutans* counts with significative differences *versus* vehicle ($p \leq 0.0012$). Additionally, biofilms treated with C135 presented less bacterium quantification than C135 + Far + F ($p = 0.0172$). However, for *C. albicans*, the treatments containing C135 + Far and C135 + Far + F showed lower colony forming units (CFUs) than other tested groups. Thus, significant statistical differences for *C. albicans* were observed for C135 + Far (*vs* C135 + F, Far, F, and V) and C135 + Far + F (*vs* Far and F) ($p \leq 0.0056$).

https://doi.org/10.1021/acsomega.2c02318
ACS Omega 2022, 7, 22773−22786

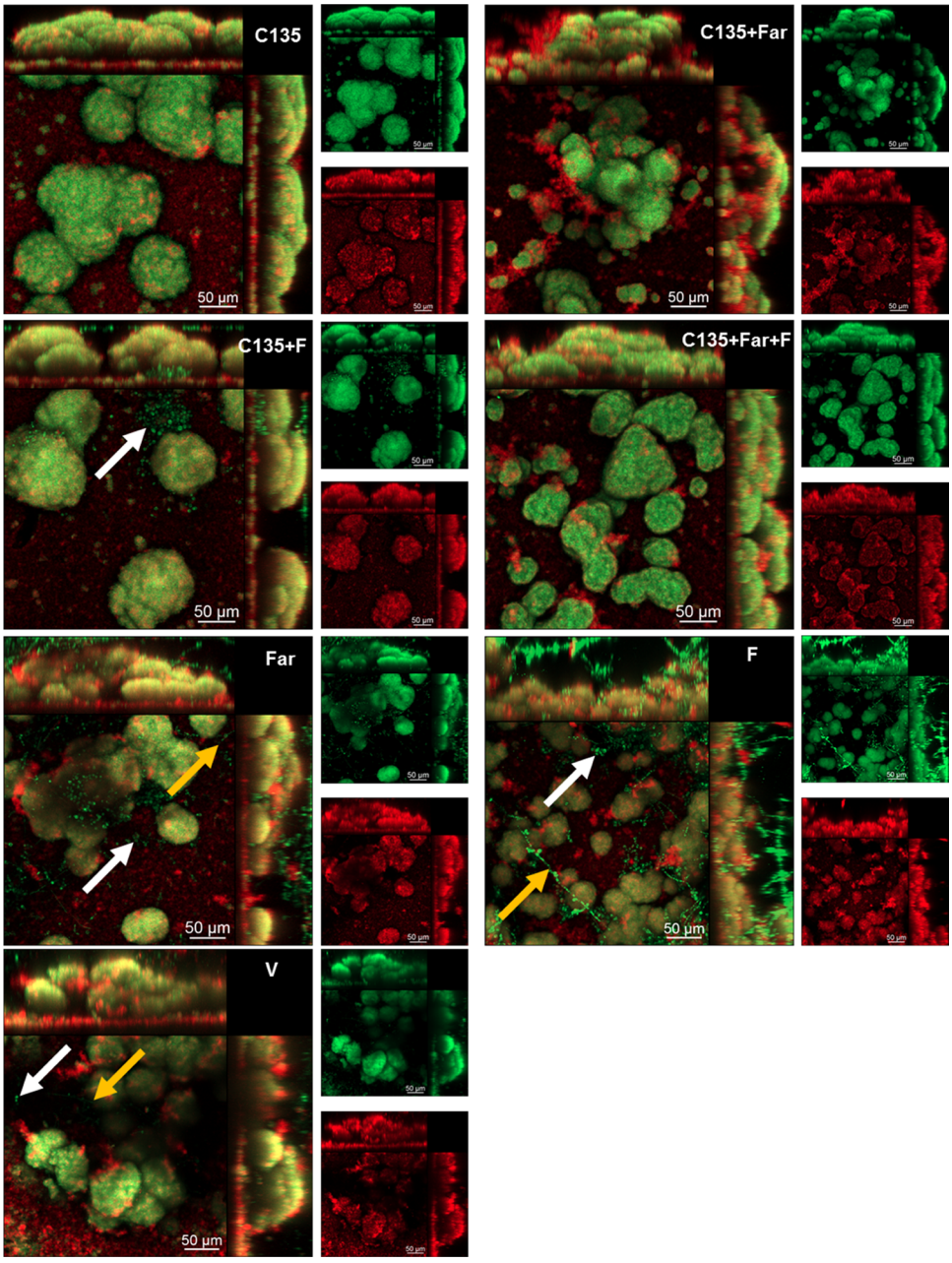

Figure 5. Representative confocal microscopy images of 43 h old *S. mutans* and *C. albicans* biofilms. Biofilms treated with compounds C135, *tt*-farnesol (Far), and sodium fluoride (F) alone or in combination (C135, C135 + Far, C135 + F, C135 + Far + F, Far, F), and vehicle or V. The arrow shows *C. albicans* cells, yeast in white and hyphae in yellow. Representative images from three different experiments. Green represents the microbial cells labeled with SYTO9, and red represents the exopolysaccharides in the extracellular matrix (labeled with Alexa Fluor 647). The larger images show the overlay of both components.

Biomass (Dry Weight) and Proteins from the Insoluble Portion of Biofilms. The biomass and proteins from the insoluble portion of biofilms data are displayed in Figure 3. The lower biomass of biofilms was recovered after treatment with C135 + Far with significant statistical differences versus all other treatments except C135 + Far + F ($p \leq 0.0051$). The same behavior was observed for biofilm proteins, where C135 + Far also presented lower quantification with significant statistical differences *versus* C135, C135 + F, F, and V ($p \leq 0.0388$).

Extracellular Matrix Components. The quantification of exopolysaccharides is represented as water-insoluble or alkali-soluble polysaccharides (ASPs) and water-soluble polysaccharides (WSPs) for each treatment group, as shown in Figure 4. C135 + Far yielded lower ASP quantification *versus* all treatments ($p \leq 0.0051$), except C135 + Far + F ($p = 0.2532$). C135 + Far + F resulted in less ASP than C135 + F and F ($p \leq 0.0372$). However, no significant differences between treatment groups were detected for WSP ($p = 0.1408$). Also, no differences were observed for proteins (soluble portion) ($p = 0.1361$) and extracellular DNA or eDNA ($p = 0.1513$) (Figure 4). Thus, the formulations C135 + Far and C135 + Far + F impacted the insoluble polysaccharides, a virulence determinant of cariogenic biofilms,[29] compared to the other matrix components. The reduced production of ASP results in less biomass (Figure 3),

https://doi.org/10.1021/acsomega.2c02318
ACS Omega 2022, 7, 22773−22786

as these components are the major ones in the matrix of cariogenic biofilms.

3D Structure. The 3D structures of *S. mutans* and *C. albicans* biofilms were acquired at 43 h and are represented in Figure 5. Biofilms treated with C135 were thicker with large and organized clusters of bacterial cells (microcolonies), but visible fungal cells were sparse. However, biofilms treated with C135 + F presented a reduced thickness and spaced-out clusters of bacterial cells surrounded by *C. albicans* cells in yeast morphology. The biofilms treated by all compounds in combination (C135 + Far + F) were ticker and organized; however, the bacterial microcolonies were smaller when compared with vehicle, and no *C. albicans* cells were visible. In the biofilms treated with C135 + F, many yeast cells were observed near the large *S. mutans* clusters. Biofilms treated with Far were smaller than those treated with F and vehicle; however, the fungi cells were visible in different morphologies.

In addition, quantification of fluorescence of biofilm components labeled with SYTO9 (both microorganisms) and Alexa Fluor 647 (bacterium-derived exopolysaccharides) by COMSTAT2 included the biomass or biovolume ($\mu m^3/\mu m^2$; the volume occupied by the fluorescence signals), maximum thickness (μm; distance from the interface disc/biofilm to the biofilm/fluid interface or until no more fluorescence is detected), and the percentage coverage areas (coverage area from the disc/biofilm interface until no more fluorescence is detected). The biomass and maximum thickness data are shown in Figure 6, and the percentage coverage areas are depicted in Figure 7.

Regarding biomass (Figure 6A), mixed ANOVA analysis, comparing as factors formulation and biofilm component demonstrated that formulation presented difference (p = 0.0005) and components also had difference (p = 0.0057), but not for both formulations *versus* components (p = 0.1950). Thus, for exopolysaccharides, the formulation C135 + F presented less biovolume *versus* F and V ($p \leq 0.0068$), followed by formulation C135 + Far + F *versus* V (p = 0.0289). Similarly, for microorganisms, the formulation that yielded the lowest biovolume was C135 + F *versus* F (p = 0.0178) and V (p = 0.0006), followed by formulation C135 + Far + F *versus* V (p = 0.0141) and C135 *versus* V (p = 0.0086).

Concerning maximum thickness (Figure 6B), mixed ANOVA analysis, comparing as factors formulation and biofilm component, demonstrated that formulation presented a difference (p = 0.0003) and components did not have a difference (p = 0.0882); also, there was no difference for formulation *versus* components (p = 0.2517). The lowest thickness was observed for exopolysaccharides and microorganisms for C135 + F *versus* C135 + Far, F, and V ($p \leq$ 0.0038 for both components).

At last, regarding the coverage area by exopolysaccharides and microorganisms (Figure 7), five formulations presented similar patterns, with two exceptions: C135 + F presented the lowest distance (which is coherent with the maximum thickness data), while V showed a higher percentage of microorganisms than exopolysaccharides in the most external layers (toward the biofilm/fluid interface).

Scanning Electronic Microscopy (SEM). The SEM images are represented in Figure 8. Biofilms treated with C135 + Far and C135 + Far + F were smaller than the vehicle (V), with fewer microbial clusters, and presented *C. albicans* only in yeast form (easily observed on 1000 and 5000× magnifications). Biofilms treated with Far showed some *C. albicans* on the initial filamentary formation (clear on 5000×) and others in yeast form above the *S. mutans* clusters. Biofilms treated with C135 and C135 + F presented all morphologies of *C. albicans*, but *S. mutans* clusters were still smaller than the vehicle control (V) and F. For V and F, the hyphal cells were scattered throughout the disc and surrounding the bacterial cells clusters, especially for V.

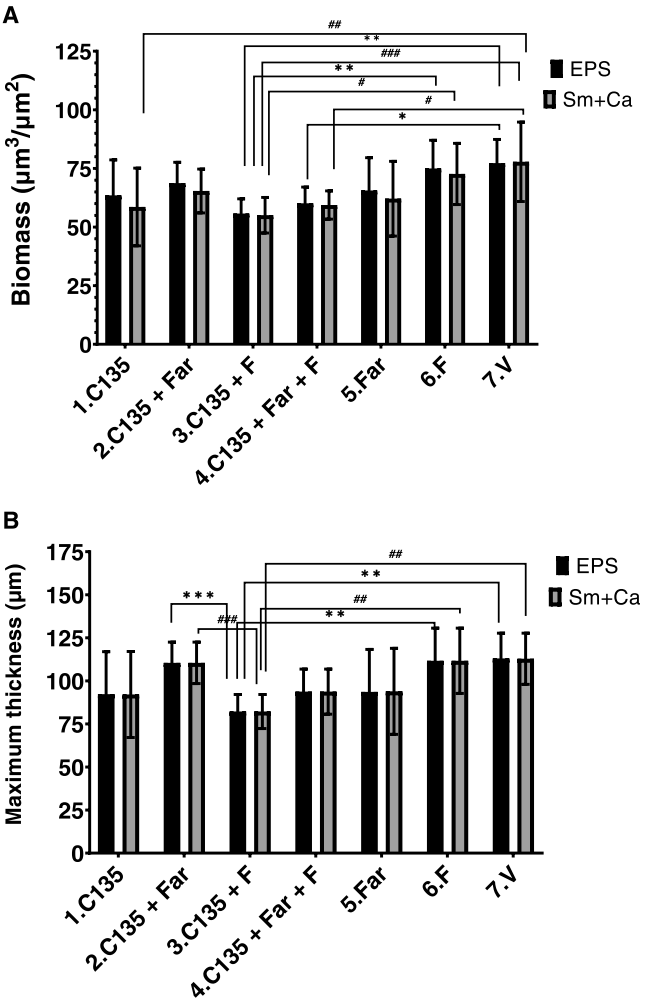

Figure 6. Biomass (A) and maximum thickness (B) of 43 h old *S. mutans* and *C. albicans* biofilms. Biofilms treated with C135, *tt*-farnesol (Far), and sodium fluoride (F) alone and in combination (1.C135; 2.C135 + Far; 3.C135 + F; 4.C135 + Far + F; 5.Far; 6.F) and 7.Vehicle or V. Data represents means and standard deviations of the exopolysaccharides from the biofilm matrix (EPS, in black) and microorganisms (*S. mutans*: Sm and *C. albicans*: Ca, in gray). Graph A represents the biomass or biovolume (top). Differences are represented by * for EPS or # for Sm + Ca: *p = 0,0289; **p = 0.0068; #$p \leq$ 0.0178; ##p = 0.0086 and ###p = 0.0006. Graph B (bottom) represents the maximum thickness of the biofilm confocal images: **$p \leq$ 0,0038; ##$p \leq$ 0.0038, ###p = 0.0036.

DISCUSSION

The formulations applied in this study presented diverse effects against *C. albicans* and *S. mutans* dual-species biofilms. Furthermore, the *in vitro* model used has extremely cariogenic conditions, such as the combination of *C. albicans* and *S. mutans* growing in the presence of sucrose;[3] hence, a strategy that can affect virulence parameters is desired because it could

https://doi.org/10.1021/acsomega.2c02318
ACS Omega 2022, 7, 22773−22786

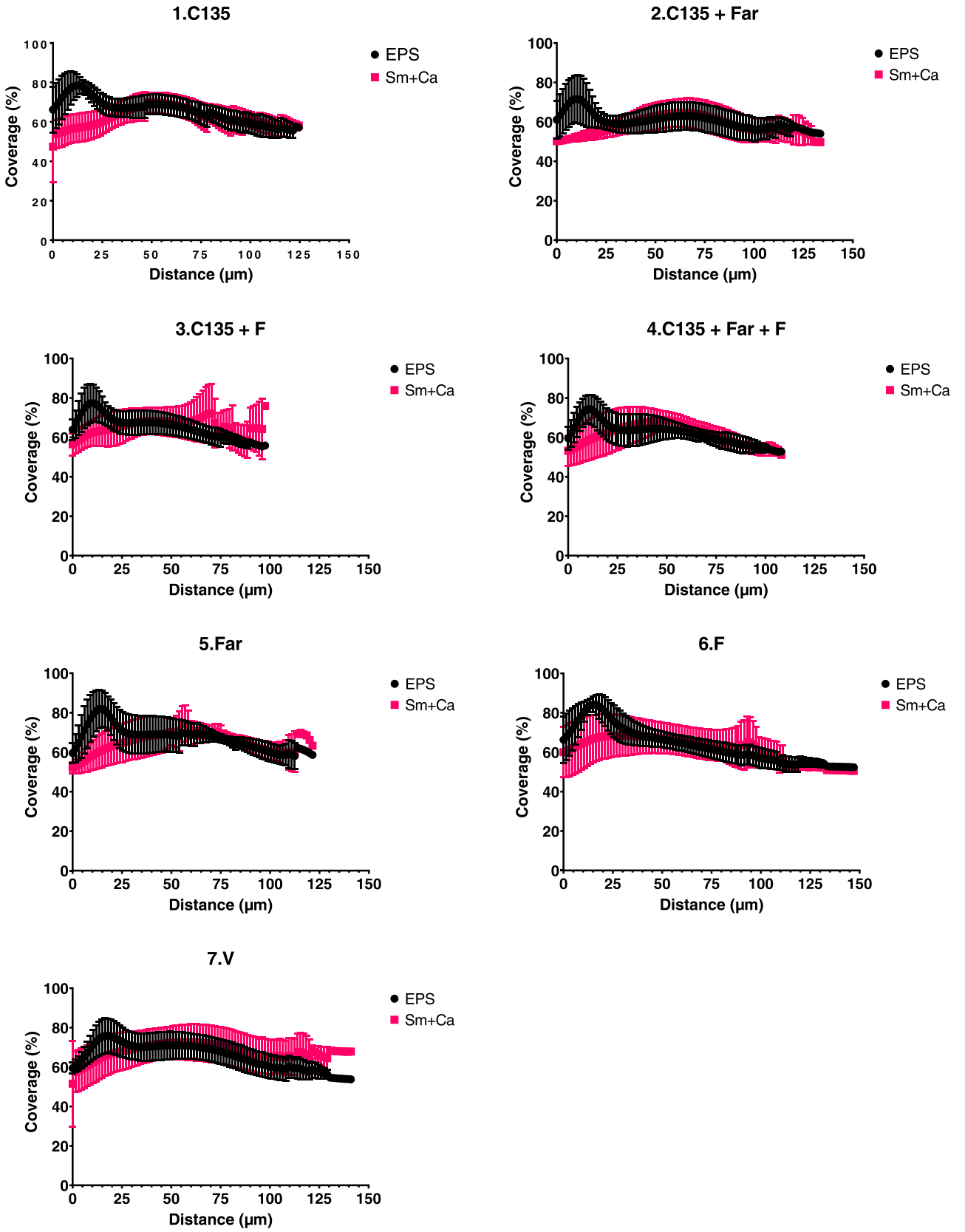

Figure 7. Data represents means and standard deviations of the coverage percentage exopolysaccharides of the biofilm matrix (EPS, in black) and microorganisms (*S. mutans*, Sm and *C. albicans*, Ca, in pink) on hydroxyapatite discs. Biofilms treated with C135, *tt*-farnesol (Far), and sodium fluoride (F) alone and in combination (1.C135; 2.C135 + Far; 3.C135 + F; 4.C135 + Far + F; 5.Far; 6.F) and 7.Vehicle or V.

be an indication of further investigation to improve the strategy for clinical application.

Among the virulence parameters, the acidogenicity of biofilms reflects the metabolization of cariogenic sugar into

https://doi.org/10.1021/acsomega.2c02318
ACS Omega 2022, 7, 22773−22786

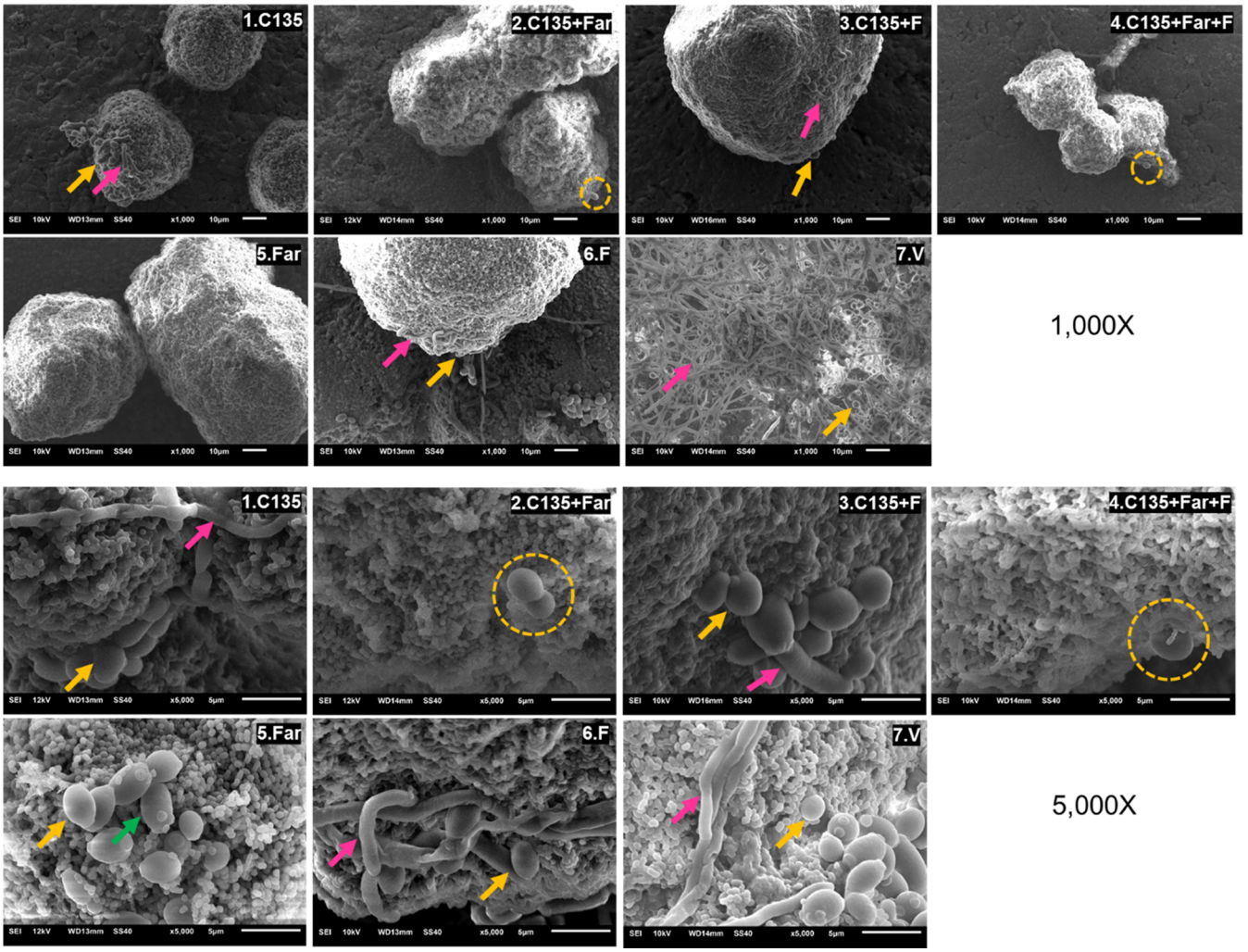

Figure 8. SEM representative images of 43 h old *S. mutans* and *C. albicans* biofilms. Biofilms treated with compounds C135, *tt*-farnesol (Far), and sodium fluoride (F) alone or in combination (C135, C135 + Far, C135 + F, C135 + Far + F, Far, F), and vehicle or V. The images were acquired on 1000 and 5000×; *C. albicans* in yeast form are identified by yellow; the initial filamentary morphology is in green, and the hyphal cells are in pink.

acids that can cause dental demineralization. A previous study of the dual-species model used here demonstrated that the pH values of spent culture medium at 19 and 43 h are more acidic (≅4.2) than at 27 h (≅4.7).[5] Here, a similar behavior was observed for biofilms treated with formulations without fluoride (C135, C135 + Far, Far, and vehicle) at 19 and 43 h, while increased pH was measured for formulations with fluoride (C135 + F, C135 + Far + F, and F) (more pronounced at 43 h; Figure S1). Thus, formulations containing fluoride can avoid a pH decrease in the culture medium, which is needed for the remineralization process to maintain teeth' enamel surface. Although all values were below the threshold for enamel demineralization (*i.e.*, pH of 5.5), at 27 h, formulations with C135 and Far presented higher pH values than other groups, and these findings could be related to a possible reduction in the virulence potential of biofilms when both compounds are associated.

Biofilms formed by *S. mutans* and *C. albicans* are more complex, structured, and exhibit an organized extracellular matrix than single-species biofilms, making both species more tolerant to environmental stresses.[5] The gene expression of microbial species regulates the mechanisms for surviving and developing biofilm. For *S. mutans*, the gene expression for oxidative stress (*nox*1) was increased when biofilms were treated with C135 + Far + F, while for *C. albicans*, all formulations with C135 led to a decrease in *SOD*1 expression (associated with fungal oxidative stress tolerance). These findings reveal that the combination of all compounds was more effective than other treatments, triggering the bacterial oxidative tolerance response since a previous study observed a reduced gene expression of *nox*1 for dual-species biofilm of *S. mutans* and *C. albicans* without treatment.[5] Thus, the decreased gene expression for the treatments containing C135 for *C. albicans* could be because of the effect of chalcones in cell wall formation and mitochondrial dysfunctions.[24] These data also confirm the antibiofilm effect of C135 for *C. albicans* observed in initial and preformed single- and dual-species biofilms after prolonged exposure to the agent.[25]

Genes *BGL2*, *FKS*1, *PHR*1, and *XOG*1 are related to *β*-1,3-glucan and *β*-1,6-glucan (*PHR*1) synthesis and are essential for the extracellular matrix construction.[12−14] In response to specific signals, *C. albicans* cells reduce the exposure of *β*-1,3-glucan on their cell surface, causing impacts on the cell wall biosynthesis.[11] Here, the *BGL2* gene showed reduced

https://doi.org/10.1021/acsomega.2c02318
ACS Omega 2022, 7, 22773−22786

expression for all treatments containing C135, Far, or when both compounds were combined. In addition, for *FKS*1, *PHR*1, *XOG*1, and *CDR*1 (important for fungal resistance) genes, the impact on *C. albicans* cells with decreased gene expression was observed for C135 + Far + F. Also, a reduced gene expression for acid stress tolerance gene *PHR*2 occurred for C135 + Far and C135 + Far + F, and a similar behavior was observed for *ERG*11 gene expression (also for C135). The *ERG*11 gene is essential for ergosterol biosynthesis that can influence membrane permeability and consequently fungal virulence.[16,18] In addition, *ERG*11 interferes with hyphal elongation,[18] corroborating with the confocal images (Figure 5, in which it was not possible to visualize the fungal cells for C135, C135 + Far, and C135 + Far + F) and with SEM images (Figure 8; C135 + Far and C135 + Far + F presented *C. albicans* cells only as yeast morphology). Thus, these findings reveal that the best effect against *C. albicans* in dual-species biofilms with *S. mutans* was observed using a formulation combining compounds that affect the biofilm construction and virulence (acid and oxidative stresses, antifungal resistance, and extracellular matrix construction).

The viable microbial population was affected by some formulations, but the log reduction was more pronounced for the fungus. *S. mutans* counting was lower when biofilms were treated with C135, C135 + Far, and Far. *C. albicans* counting was reduced by C135 + Far with or without fluoride, corroborating with the fungal gene expression. The findings of the biofilm treated with C135 + Far are also related to the biomass (insoluble dry weight), proteins (from insoluble portion), and exopolysaccharides in the matrix (mainly ASP). Meanwhile, C135 and C135 + F decrease biomass (biovolume), maximum thickness, and percentage area coverage from the confocal analysis.

Considering the ASP data, it was expected to observe the lowest exopolysaccharides biovolume (via confocal quantification) for C135 + Far, but the biovolume was the lowest for C135 + F, which presented a higher amount of ASP. A contradiction is apparent between quantifying exopolysaccharides via fluorescence (biovolume data, Figure 6) and the biochemical assay for insoluble exopolysaccharides (ASP data, Figure 4). This contradiction could be because the biochemical assay is more sensitive and quantifies the total ASP in the biofilm sample (covering all disc's surfaces) and exopolysaccharides produced by the bacterium and the fungus. In contrast, confocal analysis was performed using at least three images from one of the surfaces (*i.e.*, there is no quantification of signals in the entire biofilm sample grown on a disc at the settings performed here), and the fluorescence signal is for exopolysaccharides produced by the bacterium. Another point is that the volume occupied by the fluorescence signal could present a distinct "density"; it could be that the fluorescence is spread out for bigger microcolonies observed for C135 + Far *versus* the smallest microcolonies detected for C135 + F.

Nevertheless, C135 could be acting primarily on bacterial exopolysaccharide production[23] and fungal cells and their β-glucan metabolism on the cell wall and for the matrix.[12,13] Thus, its combination with *tt*-farnesol, which hinders fungal filamentation, could further decrease the substrate available for bacterial Gtfs binding and activity. Thus, the net result would be a biofilm with the lowest ASP and consequent lowest insoluble dry weight, as observed here.

Furthermore, on confocal images, it was challenging to observe *C. albicans* cells on biofilms treated with C135, C135 + Far, and C135 + Far + F; however, for *S. mutans*, organized clusters were present, and the fungi cells could have been immersed by the bacterial cells and extracellular matrix. In addition, yeast cells were observed for C135 + F, suggesting that the formulation affects the fungal morphology and implicates reduced biomass, thickness, and coverage of HA discs; F may potentiate the effect of C135. In addition, host-relevant conditions, including hypoxia and shifts in ambient pH, influence cell wall architecture.[24] However, the mechanisms governing β-1,3-glucan masking in *C. albicans* have proven elusive.[30]

The SEM images of biofilms confirm the effect of C135 and Far on the morphology of *C. albicans* cells, especially for treatments combining both agents (with or without F) with fewer *S. mutans* clusters and fungal cells only in yeast form. These data agree with the *C. albicans* population data and with the gene expression profiles of *BGL*2, *ERG*11, *PHR*1, and *SOD*1, indicating the effect on the cellular membrane, oxidative stresses adaptation, filamentary morphogenesis, and fungal virulence.[13−15,18]

At last, the three formulations with *tt*-farnesol (C135 + Far, C135 + Far + F, and Far) were highly cytotoxic for oral keratinocytes NOK-Si, organized as a monolayer (Figure S2). The same outcome was observed for CHX (at 0.12% as found in commercial mouthwashes), which is the gold-standard oral antimicrobial formulation. However, higher concentrations of Far against distinct cell lineages, such as fibroblasts L929 and SW480, did not present cytotoxicity;[31,32] hence, the effect observed here could be because of cell type. Moreover, topical application of *tt*-farnesol formulations at higher concentrations than the one used here did not cause oral mucosal damage in animals.[33] Thus, the current findings could be because of the monolayer of keratinocytes instead of a tridimensional tissue of oral mucosas.

C135 and *tt*-farnesol affected the *C. albicans* and *S. mutans* dual-species biofilms. Their formulations with and without fluoride affected acidogenicity, exopolysaccharide production, and the hyphal morphogenesis of *C. albicans*. However, it is still necessary to further understand the virulence mechanisms triggered in biofilms when both species are together. In addition, saliva was used for pellicle formation on HA discs, but it was not continuously present as it occurs in the oral cavity for individuals without saliva production issues. Saliva can modify the characteristics of teeth and microbial surfaces[19] and could complex the compounds, which could reduce or mask the effect of a formulation. Thus, an alternative could be the encapsulation of the compounds for controlled release[33] to circumvent the virulence and improve the effectiveness of compounds in preventing cariogenic biofilms and caries occurrence.

METHODS

Compounds and Their Combinations (Formulations Tested). Previously, our research group selected and combined compounds against single- and dual-species biofilms of *C. albicans* and S. *mutans* on 96-well plates (24 h and 48 h).[25] Also, based on pilot tests, the promising compounds are as follows: 4′-hydroxychalcone (C135): (2E)-1-(4-hydroxyphenyl)-3-phenylprop-2-en-1-one (AK Scientific, Inc.; Cat.#C135; 98% purity) and *tt*-farnesol (Far): (*E*,*E*)-3,7,11-Trimethyl-2,6,10-dodecatrien-1-ol, *trans*,*trans*-3,7,11-Trimethyl-2,6,10-dodecatrien-1-ol (Sigma-Aldrich Co., St Louis, MO; Cat.#46193; 96% purity) diluted with 84.15% ethanol (EtOH;

https://doi.org/10.1021/acsomega.2c02318
ACS Omega 2022, 7, 22773−22786

Sigma-Aldrich; Cat.#E7023) and 15% dimethyl sulfoxide (DMSO; Sigma-Aldrich; Cat.#D8418) for stock solutions at 15 mg/mL. These compounds were used alone and in combination, with and without sodium fluoride (F) (stock solution at 5000 ppm; Sigma-Aldrich; Cat.#71519). The final concentrations for both compounds (C135 and *tt*-farnesol) were 125 μg/mL based on previous data and 250 ppm for fluoride.[25,34] The test groups were the following formulations: 1. C135, 2. C135 + Far, 3. C135 + F, 4. C135 + Far + F, 5. Far, 6. F, and 7. Vehicle or V (control group: the solution used to dilute the compounds at their working concentrations: 7% EtOH + 1.25% DMSO). Chlorhexidine digluconate solution 0.12% (Sigma-Aldrich; Cat.#C9394) was used for the cytotoxicity assay (Supporting Information).

Strains and Biofilm Formation. Strains *C. albicans* SC5314 and *S. mutans* UA159 (serotype c; ATCC 700610) were plated separately on blood agar (5% sheep's blood; Laborclin, São Paulo, Brazil) and incubated for 48 h at 37 °C and 5% CO_2 (Steri-CultThermo Scientific, Waltham). Starter cultures were prepared with five colonies of each microorganism in 10 mL of culture medium [9.5 mL (2.5% tryptone and 1.5% yeast extract—TY, pH 7.0; Difco) + 0.5 mL (20% glucose): TY + 1% glucose; all of these % are w/v]. These tubes were incubated for 16 h (37 °C, 5% CO_2) and then diluted (1:20 v/v) using the same culture medium for the inoculum of each strain. The inoculum was incubated (37 °C, 5% CO_2), and each culture was used at its corresponding mid-log growth phase: *S. mutans* optical density (OD_{562nm}) 0.500 (±0.100) and *C. albicans* OD_{562nm} 0.482 (±0.058) (ELISA plate reader, Biochrom Ez, Cambourne, U.K.). The final culture for biofilm formation containing both microorganisms was prepared using TY + 1% sucrose (w/v) to yield 2×10^6 CFU/mL *S. mutans* and 2×10^4 CFU/mL *C. albicans*.[7]

Biofilms were formed on hydroxyapatite (HA) discs (2.7 ± 0.2 cm^2; Clarkson Chromatography Products, Inc., South Williamsport, PA). Wire apparatuses were used to place the HA discs vertically in 24-well plates (KASVI, China). Before the biofilm formation, the discs were coated with saliva collected by three health donors (Institutional Ethical Committee CAAE: 08189119.7.0000.5416). This saliva was stimulated (chewing a piece of parafilm), sterilized by filtration (0.2 μm aPES membrane, Rapid Flow Filter, Mexico), and prepared following a previous protocol.[35] For salivary pellicle formation, the HA discs were hydrated (sterilized Milli-Q water, 20 min), incubated in saliva (1 h, 37 °C, 75 rpm; Quimis, São Paulo, BR), and then dipped into adsorption buffer [50 mM KCl, 1 mM KPO_4, 1 mM $CaCl_2$, 1 mM $MgCl_2$, 0.1 mM PMSF (phenylmethylsulfonyl fluoride—Sigma), in dd-H_2O, pH 6.5] for washing to remove excess saliva. Next, the discs with the pellicle were treated (as described in *Treatment Regimen*) and transferred to the inoculated culture medium for biofilm formation. The biofilms were treated at 6, 21, and 29 h.

At 19 and 27 h of the experiment, biofilms were transferred to a new plate with fresh culture medium (TY + 1% sucrose) and incubated again (37 °C, 5% CO_2). After 2 h of incubation (21 and 29 h), the biofilms were treated, as described below. The spent culture medium (from 19, 27, 28, and 43 h) was used for pH analysis (Figure S1). The biofilms were grown up to 28 h for gene expression analysis and 43 h for microbial population, biomass, biochemical (matrix components: exopolysaccharides, proteins, and extracellular DNA or eDNA), and structural organization.

Treatment Regimen (Topical Application). Formulations were applied at 0, 6, 21, and 29 h. For topical application, 2 mL of each formulation (or control) was prepared on the 24-well plate. First, the discs (with salivary pellicle at 0 h, and with biofilms at 6, 21, and 29 h) were rinsed to remove the excess of saliva (after pellicle formation at 0 h) or of the culture medium (at 6, 21, and 29 h) by dipping them into adsorption buffer after pellicle or 0.89% NaCl solution during biofilm treatment. Next, these discs were submerged for 5 min into the formulations (or control), then washed using a new adsorption buffer or 0.89% NaCl solution, and transferred to the culture media, followed by incubation (37 °C, 5% CO_2).

Gene Expression Analysis. The reverse transcription-quantitative polymerase chain reaction or RT-qPCR analysis included RNA isolation, cDNA synthesis, and qPCR using specific primers for selected genes (*S. mutans*: *atpD*, *gtfB*, *nox*1, and 16S rRNA; *C. albicans*: *BGL*2, *CDR*1, *ERG*11, *PHR*1, *PHR*2, *FKS*1, *SOD*1, *XOG*1, and *RPP*2*B*).

Biofilms were processed and evaluated at 28 h. The RNA isolation protocol was established before,[36] with some modifications.[5] First, the phenol−chloroform separation method was used for RNA extraction, followed by DNAse treatments in the column (RNeasy Micro Qiagen, Germany) and solution (TURBO DNAse; Ambion) for purification. In addition, the Rneasy MinElute cleanup kit (Qiagen) was employed, followed by agarose gel electrophoresis (1%) (Ultra-Pure Invitrogen) to verify the integrity of purified total RNA. Then, the RNA quantity (260 nm) and purity (260/280) were analyzed by spectrophotometry (Nano-spectrophotometer DS-11+, Denovix).

The cDNA synthesis was performed using the iScript kit (BioRad). For +RT samples, 1 μg of total RNA (5 μL of RNA at 200 ηg/μL) was mixed with 4 μL of 5× iScript buffer, 1 μL of reverse transcriptase enzyme, and molecular-grade water to complete 20 μL (10 μL). The same reaction without reverse transcriptase enzyme was used for −RT samples.[5] The reactions were incubated [25 °C/5 min, 42 °C/30 min, 85 °C/5 min, hold at 4 °C; CFX96 thermocycler (BioRad)] and stored at −20 °C.

The cDNA samples (+RT diluted 1:5 for specific genes and 1:1000 for 16S rRNA; and −RT undiluted to ensure no DNA contamination) were amplified with specific primers, following standard protocols.[37] For qPCR reactions, 0.5 μL of cDNA was amplified with the adequate volume of 10 μM corresponding primers (Table S1), 12.5 μL of 2× SYBR Green Supermix (BioRad), and molecular-grade water up to 25 μL. The reactions were carried out according to the optimal concentration and the ideal temperature of each primer using the CFX96 (BioRad) and StepOnePlus Real-time PCR System (Applied Biosystems). Standard curves based on the PCR product were used.[38] The 16S rRNA gene act as a normalizer gene for *S. mutans*,[37] and the RPP2B (structural ribosome constituent) gene was selected for *C. albicans*;[39] however, under this experimental design, it did not work as a normalizer as observed before.[5]

The biofilm samples were obtained from a pool of four replicates per treatment in three independent experiments (n = 3).

Biofilm Processing and Analyses. At 43 h, biofilms were processed to quantify viable bacterial and fungal counts, biomass (insoluble dry weight), protein content (in the insoluble and soluble portions of the biofilms), exopolysaccharides (water-soluble polysaccharides, WSPs; and alkali-

https://doi.org/10.1021/acsomega.2c02318
ACS Omega 2022, 7, 22773−22786

soluble polysaccharides, ASPs), and eDNA in the matrix.[35,40−42] Three independent experiments were performed, where each group had two discs per treatment (n = 6).

Structural Organization of Biofilms (Confocal Microscopy). Biofilms were analyzed at 43 h via confocal microscopy. All procedures for biofilm formation and topical treatments were as described above, except that 13.4 μL of 1 mM Alexa Fluor 647 fluorophore-labeled dextrans (647/668 nm; Molecular Probes, Carlsbad, CA, EUA) was added to the culture medium to label the extracellular matrix (at 0, 19, and 27 h). At 43 h, the biofilms were dip-washed on a 24-well plate containing 0.89% NaCl and incubated in another 24-well plate containing 0.89% NaCl with 1.5 μL of SYTO9 (485/498 nm; Molecular Probes) (30 min) to label microorganisms.[5,40] After, they were dip-washed on a new 24-well plate with 0.89% NaCl and imaged.

A confocal microscope (Carl Zeiss LSM 800 with Airyscan and a GaAsp detector, Germany) was used with an EC Plan-Neofluar 20×/0.50 Oil DIC M27 objective, with laser wavelengths (488 nm, 2.10%; and 561 nm, 1.81%), with increments of 1.5 μm. The images were analyzed using ZEN Blue software to quantify the biomass, maximum thickness, and percentage of coverage area using COMSTAT2.

Three experimental occasions were performed. Two discs represented each treatment group (formulation), and three images were acquired per disc avoiding the disc's edges (n = 6). All data files were used for the quantification analyses, and a representative image from each group was selected to illustrate the findings.

Scanning Electron Microscopy (SEM). Biofilms were grown and treated as described above up to 43 h and then prepared for SEM analysis. The discs with the biofilms were washed with 0.89% NaCl, and the biofilms were fixed using glutaraldehyde solution at 2.5% (1 h at room temperature). Next, the samples were washed three times with 0.89% NaCl, dehydrated [by incubation on 70% ethanol (1×/1 h), 90% ethanol (1×/1 h), and 99% ethanol (5×/30 min)], and dried on a silica vacuum desiccator (7 days). After, the biofilms were metalized with gold (Denton Vaccum, Desc V) and the images were acquired on amplification of 1000 and 5000× in a scanning electron microscope (JEOL JSM-6610LV). Each treatment group (formulation) was represented by two discs, and at least three images of each amplification were acquired per disc.

Statistical Analyses. The quantitative data were analyzed using descriptive and inferential statistics. The Shapiro−Wilk test was applied for normality, and the Brown−Forsythe test was applied for homogeneity of variances, considering 5% of significance. Analyses were performed using one-way or mixed ANOVA tests, followed by Tukey's post-test (Prism 9 software, GraphPad Software, Inc., 2021). In addition, qualitative and descriptive analyses of confocal and scanning electron microscopy images were performed.

■ ASSOCIATED CONTENT

Supporting Information

The Supporting Information is available free of charge at https://pubs.acs.org/doi/10.1021/acsomega.2c02318.

Additional methodological description and results regarding primes used (Table S1), pH of the spent culture medium (Figure S1), and cytotoxicity activity (Figure S2) (PDF)

■ AUTHOR INFORMATION

Corresponding Author

Marlise I. Klein − *Department of Dental Materials and Prosthodontics, São Paulo State University (Unesp), School of Dentistry, Araraquara 14801-903, Brazil;* Present Address: Department of Oral Diagnosis, Piracicaba Dental School, State University of Campinas, Piracicaba 13414-903, SP, Brazil; orcid.org/0000-0002-7916-1557; Phone: 55 16 3301 6410; Email: marlise.klein@unesp.br

Authors

Carmélia I. Lobo − *Department of Dental Materials and Prosthodontics, São Paulo State University (Unesp), School of Dentistry, Araraquara 14801-903, Brazil*

Paula A. Barbugli − *Department of Dental Materials and Prosthodontics, São Paulo State University (Unesp), School of Dentistry, Araraquara 14801-903, Brazil*

Guilherme Roncari Rocha − *Department of Dental Materials and Prosthodontics, São Paulo State University (Unesp), School of Dentistry, Araraquara 14801-903, Brazil*

Complete contact information is available at: https://pubs.acs.org/10.1021/acsomega.2c02318

Author Contributions

K.M.I. conceptualized and designed the study. L.C.I.V., R.G.R., B.P.A., and K.M.I. performed the experiments and acquired the data. L.C.I.V. and K.M.I. analyzed and interpreted the data. L.C.I.V. drafted the manuscript. All authors contributed to the manuscript and approved the submitted version.

Funding

This research was supported by a research grant from the National Council for Scientific and Technological Development (CNPq #409668/2018-4) to M.I.K. and scholarships (CNPq #141316/2020-9 and the Coordination of Superior Level Staff Improvement—CAPES #001) to C.I.V.L. In addition, the São Paulo Research Foundation provided a scholarship (FAPESP #2018/01429-4) to G.R.R. However, the funding body had no role in the design of the study or collection, analysis, and interpretation of data and in writing the manuscript.

Notes

The authors declare no competing financial interest.

■ ACKNOWLEDGMENTS

The authors are thankful to CNPq, CAPES, and FAPESP for grant and scholarship funding. The present research is part of the Ph.D. thesis by C.I.V.L.

■ REFERENCES

(1) Selwitz, R. H.; Ismail, A. I.; Pitts, N. B. Dental caries. *Lancet* **2007**, *369*, 51−59.

(2) Anil, S.; Anand, P. S. Early Childhood Caries: Prevalence, Risk Factors, and Prevention. *Front. Pediatr.* **2017**, *5*, No. 157.

(3) Bowen, W. H.; Burne, R. A.; Wu, H.; Koo, H. Oral Biofilms: Pathogens, Matrix, and Polymicrobial Interactions in Microenvironments. *Trends Microbiol.* **2018**, *26*, 229−242.

(4) Emami, E.; de Souza, R. F.; Kabawat, M.; Feine, J. S. The impact of edentulism on oral and general health. *Int. J. Dent.* **2013**, *2013*, No. 498305.

(5) Lobo, C. I. V.; Rinaldi, T. B.; Christiano, C. M. S.; Leite, L. S.; Barbugli, P. A.; Klein, M. I. Dual-species biofilms of *Streptococcus mutans* and *Candida albicans* exhibit more biomass and are mutually

beneficial compared with single-species biofilms. *J. Oral Microbiol.* **2019**, *11*, No. 1581520.
(6) Gregoire, S.; Xiao, J.; Silva, B. B.; Gonzalez, I.; Agidi, P. S.; Klein, M. I.; Ambatipudi, K. S.; Rosalen, P. L.; Bauserman, R.; Waugh, R. E.; Koo, H. Role of glucosyltransferase B in interactions of *Candida albicans* with *Streptococcus mutans* and with an experimental pellicle on hydroxyapatite surfaces. *Appl. Environ. Microbiol.* **2011**, *77*, 6357−6367.
(7) Falsetta, M. L.; Klein, M. I.; Colonne, P. M.; Scott-Anne, K.; Gregoire, S.; Pai, C. H.; Gonzalez-Begne, M.; Watson, G.; Krysan, D. J.; Bowen, W. H.; Koo, H. Symbiotic relationship between *Streptococcus mutans* and *Candida albicans* synergizes virulence of plaque biofilms *in vivo*. *Infect Immun.* **2014**, *82*, 1968−1981.
(8) Bowen, W. H.; Koo, H. Biology of *Streptococcus mutans*-derived glucosyltransferases: Role in extracellular matrix formation of cariogenic biofilms. *Caries Res.* **2011**, *45*, 69−86.
(9) Lemos, J. A.; Burne, R. A. A model of efficiency: stress tolerance by *Streptococcus mutans*. *Microbiology* **2008**, *154*, 3247−3255.
(10) Kuhnert, W. L.; Zheng, G.; Faustoferri, R. C.; Quivey, R. G., Jr. The F-ATPase operon promoter of *Streptococcus mutans* is transcriptionally regulated in response to external pH. *J. Bacteriol.* **2004**, *186*, 8524−8528.
(11) Islam, B.; Khan, S. N.; Khan, A. U. Dental caries: from infection to prevention. *Med. Sci. Monit.* **2007**, *13*, RA196−203.
(12) Fonzi, W. A. PHR1 and PHR2 of *Candida albicans* encode putative glycosidases required for proper cross-linking of beta-1,3- and beta-1,6-glucans. *J. Bacteriol.* **1999**, *181*, 7070−7079.
(13) Vediyappan, G.; Rossignol, T.; d'Enfert, C. Interaction of *Candida albicans* biofilms with antifungals: transcriptional response and binding of antifungals to beta-glucans. *Antimicrob Agents Chemother.* **2010**, *54*, 2096−2111.
(14) Taff, H. T.; Nett, J. E.; Zarnowski, R.; Ross, K. M.; Sanchez, H.; Cain, M. T.; Hamaker, J.; Mitchell, A. P.; Andes, D. R. A Candida biofilm-induced pathway for matrix glucan delivery: implications for drug resistance. *PLoS Pathog.* **2012**, *8*, No. e1002848.
(15) Zhu, J.; Krom, B. P.; Sanglard, D.; Intapa, C.; Dawson, C. C.; Peters, B. M.; Shirtliff, M. E.; Jabra-Rizk, M. A. Farnesol-induced apoptosis in *Candida albicans* is mediated by Cdr1-p extrusion and depletion of intracellular glutathione. *PLoS One* **2011**, *6*, No. e28830.
(16) White, T. C.; Holleman, S.; Dy, F.; Mirels, L. F.; Stevens, D. A. Resistance mechanisms in clinical isolates of *Candida albicans*. *Antimicrob. Agents Chemother.* **2002**, *46*, 1704−1713.
(17) Jordão, C. C.; Klein, M. I.; Carmello, J. C.; Dias, L. M.; Pavarina, A. C. Consecutive treatments with photodynamic therapy and nystatin altered the expression of virulence and ergosterol biosynthesis genes of a fluconazole-resistant *Candida albicans in vivo*. *Photodiagn. Photodyn. Ther.* **2021**, *33*, No. 102155.
(18) Wu, Y.; Wu, M.; Wang, Y.; Chen, Y.; Gao, J.; Ying, C. ERG11 couples oxidative stress adaptation, hyphal elongation and virulence in *Candida albicans*. *FEMS Yeast Res.* **2018**, *18*, No. foy057.
(19) Liu, Y.; Ren, Z.; Hwang, G.; Koo, H. Therapeutic Strategies Targeting Cariogenic Biofilm Microenvironment. *Adv. Dent Res.* **2018**, *29*, 86−92.
(20) Pitts, N. B.; Zero, D. T.; Marsh, P. D.; Ekstrand, K.; Weintraub, J. A.; Ramos-Gomez, F.; Tagami, J.; Twetman, S.; Tsakos, G.; Ismail, A. Dental caries. *Nat. Rev. Dis. Primers.* **2017**, *3*, No. 17030.
(21) Marquis, R. E.; Clock, S. A.; Mota-Meira, M. Fluoride and organic weak acids as modulators of microbial physiology. *FEMS Microbiol. Rev.* **2003**, *26*, 493−510.
(22) Brookes, Z. L. S.; Bescos, R.; Belfield, L. A.; Ali, K.; Roberts, A. Current uses of chlorhexidine for management of oral disease: a narrative review. *J. Dent.* **2020**, *103*, No. 103497.
(23) Nijampatnam, B.; Casals, L.; Zheng, R.; Wu, H.; Velu, S. E. Hydroxychalcone inhibitors of *Streptococcus mutans* glucosyltransferases and biofilms as potential anticaries agents. *Bioorg. Med. Chem. Lett.* **2016**, *26*, 3508−3513.
(24) Al Aboody, M. S.; Mickymaray, S. Anti-Fungal Efficacy and Mechanisms of Flavonoids. *Antibiotics* **2020**, *9*, No. 45.
(25) Lobo, C. I. V.; Lopes, A. C. U. dA.; Klein, M. I. Compounds with Distinct Targets Present Diverse Antimicrobial and Antibiofilm Efficacy against *Candida albicans* and *Streptococcus mutans*, and Combinations of Compounds Potentiate Their Effect. *J. Fungi* **2021**, *7*, No. 340.
(26) Koo, H.; Schobel, B.; Scott-Anne, K.; Watson, G.; Bowen, W. H.; Cury, J. A.; Rosalen, P. L.; Park, Y. K. Apigenin and *tt*-farnesol with fluoride effects on *S. mutans* biofilms and dental caries. *J. Dent. Res.* **2005**, *84*, 1016−1020.
(27) Falsetta, M. L.; Klein, M. I.; Lemos, J. A.; Silva, B. B.; Agidi, S.; Scott-Anne, K. K.; Koo, H. Novel antibiofilm chemotherapy targets exopolysaccharide synthesis and stress tolerance in *Streptococcus mutans* to modulate virulence expression in vivo. *Antimicrob. Agents Chemother.* **2012**, *56*, 6201−6211.
(28) Rocha, G. R.; Florez Salamanca, E. J.; de Barros, A. L.; Lobo, C. I. V.; Klein, M. I. Effect of *tt*-farnesol and myricetin on *in vitro* biofilm formed by *Streptococcus mutans* and *Candida albicans*. *BMC Complement Altern Med.* **2018**, *18*, No. 61.
(29) Koo, H.; Falsetta, M. L.; Klein, M. I. The exopolysaccharide matrix: a virulence determinant of cariogenic biofilm. *J. Dent Res.* **2013**, *92*, 1065−1073.
(30) Childers, D. S.; Avelar, G. M.; Bain, J. M.; Pradhan, A.; Larcombe, D. E.; Netea, M. G.; Erwig, L. P.; Gow, N. A. R.; Brown, A. J. P. Epitope Shaving Promotes Fungal Immune Evasion. *mBio* **2020**, *11*, No. e00984.
(31) Chávez-Andrade, G. M.; Tanomaru-Filho, M.; Rodrigues, E. M.; Gomes-Cornélio, A. L.; Faria, G.; Bernardi, M. I. B.; Guerreiro-Tanomaru, J. M. Cytotoxicity, genotoxicity and antibacterial activity of poly(vinyl alcohol)-coated silver nanoparticles and farnesol as irrigating solutions. *Arch. Oral Biol.* **2017**, *84*, 89−93.
(32) Nikoomanesh, F.; Roudbarmohammadi, S.; Khoobi, M.; Haghighi, F.; Roudbary, M. Design and synthesis of mucoadhesive nanogel containing farnesol: investigation of the effect on HWP1, SAP6 and Rim101 genes expression of *Candida albicans in vitro*. *Artif. Cells Nanomed. Biotechnol.* **2019**, *47*, 64−72.
(33) Horev, B.; Klein, M. I.; Hwang, G.; Li, Y.; Kim, D.; Koo, H.; Benoit, D. S. pH-activated nanoparticles for controlled topical delivery of farnesol to disrupt oral biofilm virulence. *ACS Nano* **2015**, *9*, 2390−2404.
(34) Zero, D. T. Dentifrices, mouthwashes, and remineralization/caries arrestment strategies. *BMC Oral Health.* **2006**, *6*, No. S9.
(35) Lemos, J. A.; Abranches, J.; Koo, H.; Marquis, R. E.; Burne, R. A. Protocols to study the physiology of oral biofilms. *Methods Mol. Biol.* **2010**, *666*, 87−102.
(36) Cury, J. A.; Koo, H. Extraction and purification of total RNA from *Streptococcus mutans* biofilms. *Anal Biochem.* **2007**, *365*, 208−214.
(37) Klein, M. I.; Xiao, J.; Lu, B.; Delahunty, C. M.; Yates, J. R., III; Heydorn, A.; Koo, H. *Streptococcus mutans* protein synthesis during mixed-species biofilm development by high-throughput quantitative proteomics. *PLoS One* **2012**, *7*, No. e45795.
(38) Yin, J. L.; Shackel, N. A.; Zekry, A.; McGuinness, P. H.; Richards, C.; Putten, K. V.; McCaughan, G. W.; Eris, J. M.; Bishop, G. A. Real-time reverse transcriptase-polymerase chain reaction (RT-PCR) for measurement of cytokine and growth factor mRNA expression with fluorogenic probes or SYBR Green I. *Immunol. Cell Biol.* **2001**, *79*, 213−221.
(39) Nailis, H.; Coenye, T.; Van Nieuwerburgh, F.; Deforce, D.; Nelis, H. J. Development and evaluation of different normalization strategies for gene expression studies in *Candida albicans* biofilms by real-time PCR. *BMC Mol. Biol.* **2006**, *7*, No. 25.
(40) Klein, M. I.; Xiao, J.; Heydorn, A.; Koo, H. An analytical toolbox for comprehensive biochemical, structural and transcriptome evaluation of oral biofilms mediated by mutans streptococci. *J. Vis. Exp.* **2011**, *47*, 2512.
(41) Dubois, M.; Gilles, K. A.; Hamilton, J. K.; Rebers, P. A.; Smith, F. Colorimetric method for determination of sugars and related substances. *Anal Chem.* **1956**, *28*, 350−356.

https://doi.org/10.1021/acsomega.2c02318
ACS Omega 2022, 7, 22773−22786

(42) Castillo Pedraza, M. C.; Novais, T. F.; Faustoferri, R. C.; Quivey, R. G., Jr.; Terekhov, A.; Hamaker, B. R.; Klein, M. I. Extracellular DNA and lipoteichoic acids interact with exopolysaccharides in the extracellular matrix of *Streptococcus mutans* biofilms. *Biofouling* **2017**, *33*, 722−740.

https://doi.org/10.1021/acsomega.2c02318
ACS Omega 2022, 7, 22773−22786